TECHNICAL REPORT RL-80-3

IMPROVING A REAL TIME ACOUSTICAL HOLOGRAPHIC SYSTEM FOR FLAW DETECTION

W. F. Swinson
Auburn University
Auburn, Alabama
for
Ground Equipment and Missile Structures Directorate
US Army Missile Laboratory

1 October 1979

U.S. ARMY MISSILE COMMAND
Redstone Arsenal, Alabama 35809

REPORT DOCUMENTATION PAGE		READ INSTRUCTIONS BEFORE COMPLETING FORM
1. REPORT NUMBER RL -80-3	2. GOVT ACCESSION NO.	3. RECIPIENT'S CATALOG NUMBER
4. TITLE (and Subtitle) IMPROVING A REAL TIME ACOUSTICAL HOLOGRAPHIC SYSTEM FOR FLAW DETECTION		5. TYPE OF REPORT & PERIOD COVERED Technical Report
		6. PERFORMING ORG. REPORT NUMBER
7. AUTHOR(s) W. F. Swinson (Auburn University)		8. CONTRACT OR GRANT NUMBER(s)
9. PERFORMING ORGANIZATION NAME AND ADDRESS Commander US Army Missile Command ATTN: DRSMI-RL Redstone Arsenal, Alabama 35809		10. PROGRAM ELEMENT, PROJECT, TASK AREA & WORK UNIT NUMBERS
11. CONTROLLING OFFICE NAME AND ADDRESS Commander US Army Missile Command ATTN: DRSMI-RPT Redstone Arsenal, Alabama 35809		12. REPORT DATE 1 October 1979
		13. NUMBER OF PAGES 34
14. MONITORING AGENCY NAME & ADDRESS(if different from Controlling Office)		15. SECURITY CLASS. (of this report) Unclassified
		15a. DECLASSIFICATION/DOWNGRADING SCHEDULE

16. DISTRIBUTION STATEMENT (of this Report)

Approved for public release; distribution unlimited.

17. DISTRIBUTION STATEMENT (of the abstract entered in Block 20, if different from Report)

18. SUPPLEMENTARY NOTES

This work was accomplished through the Laboratory Research Cooperative Program (LRCP) between Dr. W. F. Swinson of the Department of Mechanical Engineering, Auburn University, and the US Army Missile Command.

19. KEY WORDS (Continue on reverse side if necessary and identify by block number)

Real Time	Optical Reconstruction
Acoustical Holography	Flaw Detection
Thermoplastic	Spatial Filter

20. ABSTRACT (Continue on reverse side if necessary and identify by block number)

This report documents work performed to improve the acoustical imaging capability of an acoustical holographic system for flaw detection. Included in the report is a mathematical model of the acoustical system and the results of the experimental effort to improve it. Added improvements include new plexiglas acoustical lenses, a lens gymbal mount, object gymbal mount, and acoustical thermoplastic memory. An attempt to use glycerine as a new acoustical couplant media is also reported. Work is also reported about the generation of acoustical real time speckle interferograms using the system.

DD FORM 1473 ᴸJAN 73   EDITION OF 1 NOV 65 IS OBSOLETE

CONTENTS

1

ILLUSTRATIONS

ILLUSTRATIONS (Concluded)

I. INTRODUCTION

The objective of the effort reported in this report was to improve the capability of the real time acoustical holographic system to detect, locate, and size subsurface flaws in missile components.

The basic system is shown in *Figure 1*. A discussion of this system is included in a report from Irelan, et al. [1]

II. THEORY

A mathematical model is included in this report to assist in understanding the acoustical system. Consider the surface of the water shown in *Figure 2*; the surface disturbance, $\bar{P}_{AO}$, due to the object wave is (note: only the real part of the complex quantities represent the disturbances)

$$\bar{P}_{AO} = \bar{P}_O \, e^{i(w_A t + \phi_{AO})} \tag{1}$$

where

$\bar{P}_O$ = the maximum amplitude of the object wave at the fluid surface (related to pressure induced into the model and model characteristics)

w_A = acoustic frequency, and

ϕ_{OA} = acoustic phase of object wave arriving at surface and is a function of x, y.

The disturbance of the surface due to the reference wave is

$$\bar{P}_{AR} = \bar{P}_R \, e^{i(w_A t + \phi_{AR})} \tag{2}$$

where

$\bar{P}_R$ = maximum amplitude of the reference wave.

ϕ_{AR} = acoustic phase of the reference wave at the water surface and is a function of x, y.

---

1. Irelan, V.G., Mullinix, B. R., Castle, J. G., "Real Time Acoustical Holography Systems," US Army Missile Research and Development Command, Technical Report T-78-10, Redstone Arsenal, Alabama 35809, October 1977.
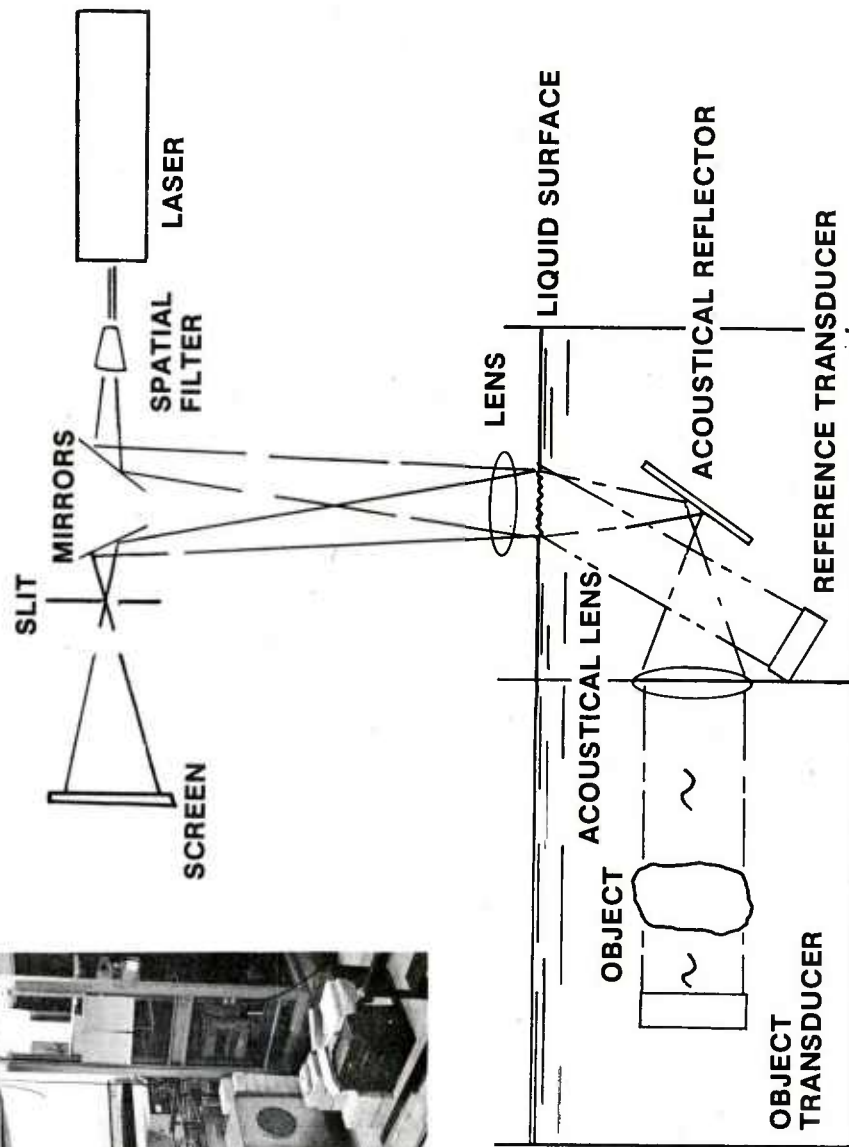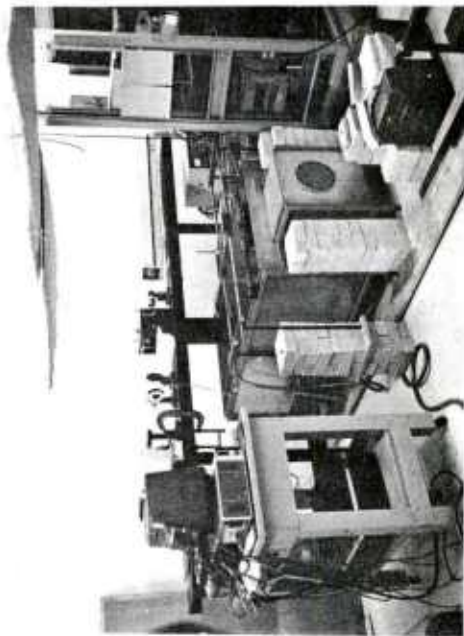
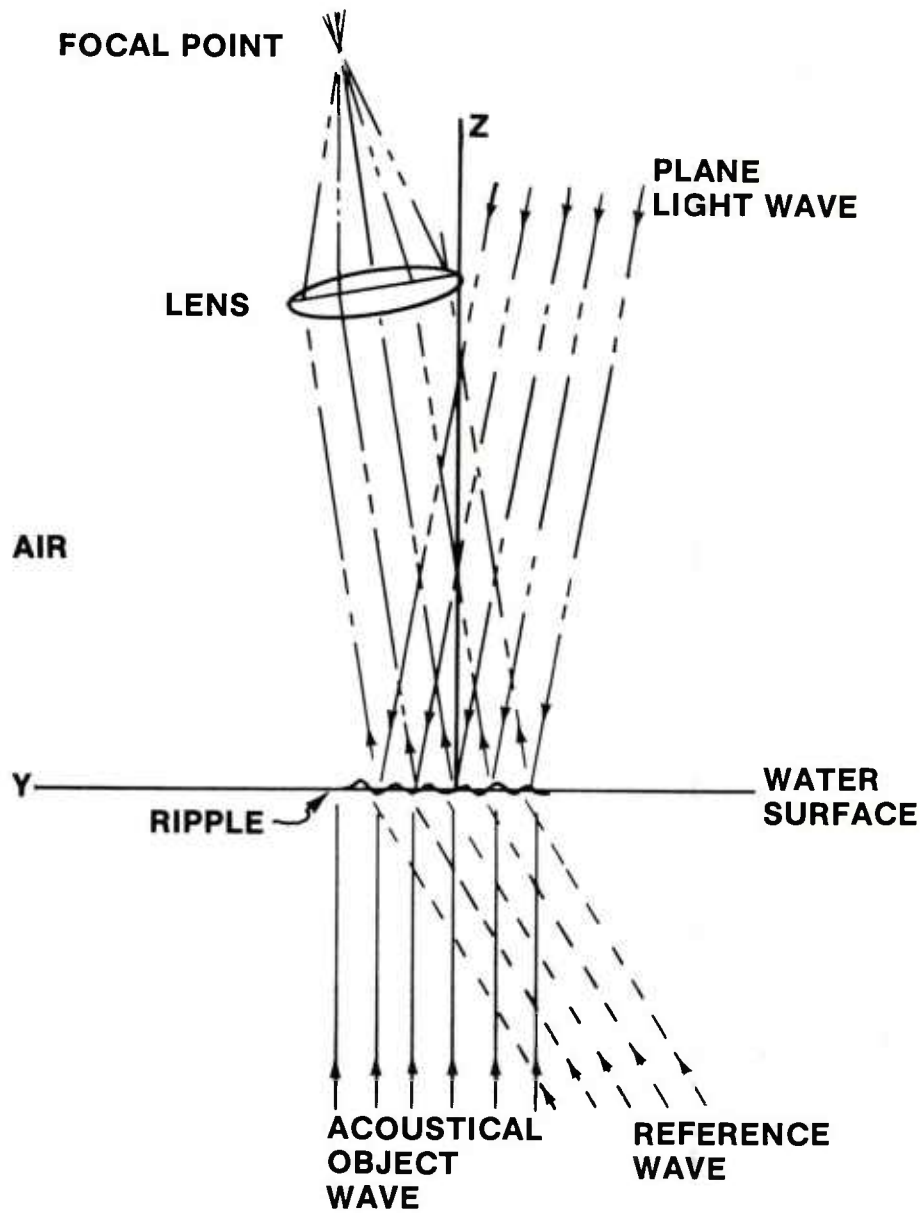Figure 1. Acoustical holography layout.

Figure 2.   Acoustical surface.

The resulting surface disturbance due to the two disturbances interfering is

$$\bar{P} = \bar{P}_{AO} + \bar{P}_{AR} \qquad (3)$$

The total disturbance intensity (which is proportional to the ripple height on the surface) is

$$I = \bar{P} \cdot \bar{P}^* \qquad (4)$$

where (*) denotes the complex conjugate. Equation (4) in expanded form is

$$I = \left[\bar{P}_O e^{i(w_A t + \phi_{AO})} + \bar{P}_R e^{i(w_A t + \phi_{AR})} \right] \cdot$$

$$\left[\bar{P}_O e^{-i(w_A t + \phi_{AO})} + \bar{P}_R e^{-i(w_A t + \phi_{AR})} \right]$$

or

$$I = P_O^2 + P_R^2 + P_O P_R e^{i(\phi_{AO} - \phi_{AR})} + P_O P_R e^{-i(\phi_{AO} - \phi_{AR})} \qquad (5)$$

With the assumption that the surface displacement is proportional to the disturbance intensity, then

$$Z = C_1 \left[P_O^2 + P_R^2 + 2 P_O P_R \cos(\phi_{AO} - \phi_{AR}) \right] \qquad (6)$$

One "ray" of light at the lens focal point changes its path length by 2Z (assuming small incident and reflecting angles); thus the optical disturbance at the focal point is

$$\bar{E} = \bar{A} \, e^{i(w_L t + \phi_L)} e^{i 4\pi z / \lambda_L} \qquad (7)$$

where

$\bar{A}$ = maximum amplitude of the optical disturbance,

w_L = light wave frequency,

ϕ_L = light wave phase, and

λ_L = light wave length.

8

Equation (7) in expanded form is

$$\bar{E} = \bar{A}\, e^{i(w_L t + \phi_L)}\, e^{i(4\pi/\lambda_L)}\, P_O^2 +$$

$$P_R^2 + 2P_O P_R \cos(\phi_{AO} + \phi_{AR})\, C_1 \tag{8}$$

To assist in interpreting this result the Bessel identity

$$e^{i\, x\, \cos\,\theta} = \sum_{n=-\infty}^{\infty} i^n\, j_n(x)\, e^{-i\, n\, \theta} \tag{9}$$

is helpful. Thus Equation (8) becomes

$$\bar{E} = \bar{A}\, e^{i(w_L t + \phi_L)}\, e^{i(4\pi/\lambda_L)(P_O^2 + P_R^2)C_1} \sum_{n=\infty}^{n=\infty} i^n j_n$$

$$\cdot \left[C_1 (8\pi/\lambda_L)\, P_O P_R \right] e^{-i\, n(\phi_{AO} - \phi_{AR})} \tag{10}$$

with "n" denoting diffraction orders $0, \pm 1, \pm 2, \text{-----}$.

The diffraction orders are

$$\bar{E}_O = \bar{A}\, e^{i(w_L t + \phi_L)}\, e^{i(4\pi/\lambda_L)(P_O^2 + P_R^2)C_1}\, j_O$$

$$\cdot \left[C_1 (8\pi/\lambda_L)\, P_O P_R \right]$$

$$\bar{E}_1 = \bar{A}\, e^{i(w_L t + \phi_L)}\, e^{i\, C_1 (4\pi/\lambda_L)(P_O^2 + P_R^2)}\, i\, j_1$$

$$\cdot \left[C_1 (8\pi/\lambda_L)\, P_O P_R \right] e^{-i(\phi_{AO} - \phi_{AR})} \tag{11}$$

$$\cdot$$
$$\cdot$$
$$\cdot$$

9

Hildebrand and Brenden "Introduction to Acoustical Holography," New York: Plenum Press, 1972 suggest that the argument of the Bessel function, $C_1(8\pi/\lambda_L) P_O P_R$, is very small in which case j_o approaches "1" and j_1 approaches the argument value of $C_1(8\pi/\lambda_L) P_O P_R$. This result seems plausible as diffraction orders can be seen at the focal plane and are illustrated in *Figure 3*. With the above assumption

$$\bar{E}_O = \bar{A}\, e^{i(w_L t + \phi_L)}\, e^{i(4\pi/\lambda_L)C_1(P_O^2 + P_R^2)}$$

$$\bar{E}_1 = i\, \bar{A}\, e^{i(w_L t + \phi_L)}\, e^{i(4\pi/\lambda_L)C_1(P_O^2 + P_R^2)}$$

$$\cdot\left[C_1(\pi 8/\lambda_L)\, P_O P_R\right] e^{-i(\phi_{AO} - \phi_{AR})} \tag{12}$$

$\bullet$

$\bullet$

$\bullet$

the intensities are

$$I_O = A^2$$

$$\tag{13}$$

$$I_1 = A^2\, C_1(\pi 8/\lambda_L)\, P_R^2 + P_O^2$$

$\bullet$

$\bullet$

$\bullet$

The predictions from Equation (13) suggest that the zero order does not contain information directly proportional to the acoustic object beam. However, recall that the mathematical description is for one "ray" and, since the surface ripple modulates the light beam, then some information relative to the object would be expected in the zero order beam. In blocking the zero order, the other diffraction orders are directly proportional to the acoustic object beam intensity as seen from Equation (13). Note that without an acoustic reference no diffractions orders are predicted, which is observed experimentally. *Figure 4* is the result of the zero order beam with no reference of two bars. For this result the object power was fully on. *Figure 5* is the result of blocking the zero order beam and including a reference beam. The object power for this was about one half maximum. There is some argument that *Figure 4* is a Gabor hologram, but the size is distorted and may only be an obstruction to the object transducer.

SECOND
FIRST
ZERO ORDER

FOCAL PLANE
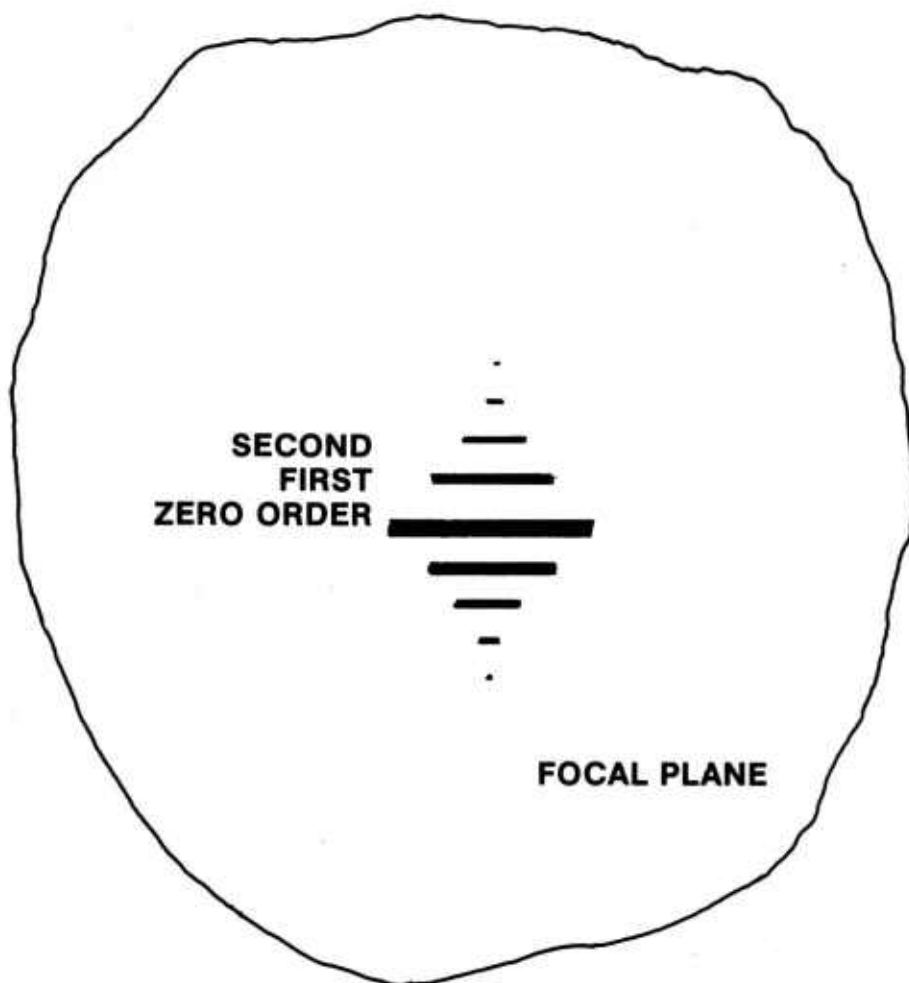
Figure 3. Diffraction orders.

11
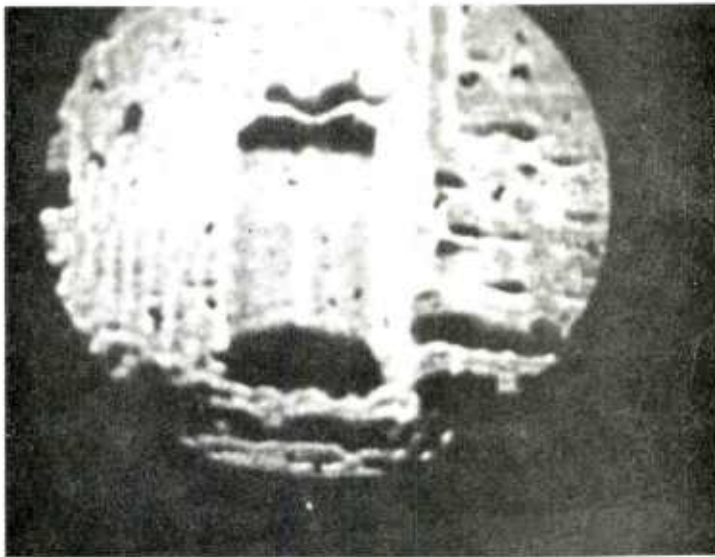
Figure 4.   Object beam only.
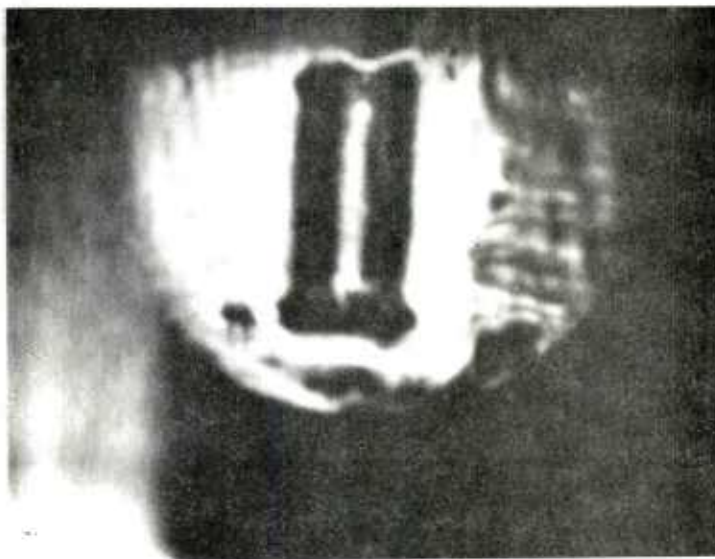
**Figure 5.   Hologram from higher order diffraction patterns.**

III.   EXPERIMENTATION

A couplant other than water was investigated. Glycerine was the material investigated. In going from water to steel 86 percent of the energy is reflected and 14 percent transmitted. In going from glycerine to steel 78 percent is reflected and 22 percent is transmitted. These numbers are for normal incidence. This suggests that 50 percent more transmitted energy is present in a model when using glycerine rather than water as an immersion fluid. This was experienced in trying the glycerine as an immersion fluid; however, the surface tension was so much greater than water that a ripple pattern on the surface could not be imaged. The glycerine was mixed with water and at 30 percent glycerine, ripple patterns were evident on the surface; however another problem came up. Even though the mixture looked uniform, when imaging the object dark and bright lines there was considerable scatter of the acoustical beam since the water and glycerine did not form a homogeneous mixture. There is still the possibility of adding detergent to reduce surface tension and promote a homogeneous mixture. This was not tried due to the lack of time. The glycerine had some beneficial effects in that it prevented rust and also damped out fluid motion. Another suggestion would be to try ethylene glycol; while it does not significantly increase the transmitted energy, it does retard rust.

A different lens was tried. Two lenses were made from plexiglas. The lenses were flat on one side and spherically concave on the other side. The concept for this design was to increase the energy input through the lens by having one surface the flat surface, and the first surface essentially perpendicular to the acoustical beam propagation path. Also lens distortion would be less because of the rigidity of the lens compared to a liquid lens. One lens had a radius of curvature of 2.250 inches and the other 4.50 inches. One of the lens and its holder is shown in *Figure 6*. To illustrate the use of the lens and other concepts in this report a target shown in *Figure 7* was used. The bars are approximately 1.5 inches long and the wider bars are about 0.35 inch wide. The target consists of black paper tape like material for the bars glued on a 0.25 inch thick piece of plexiglas. Also a flaw type model is used in some later examples. The flaw model is shown in *Figure 8* and consists of a "teflon flaw" about .5 inch by one inch sandwiched between steel and a slip silica material. The steel is five inches by five inches by 0.1 inch and is bonded to a five inch by five inch by 0.4 inch silica material.

Note that the lens holder has the capability of motion or adjustment in three directions and also rotation about the vertical axis. This holder allows the lens to be adjusted to its aligned position. Further, some control is possible on the object distance and image distance from the lens. The focal point for the acoustical lens can be calculated from thin lens equation
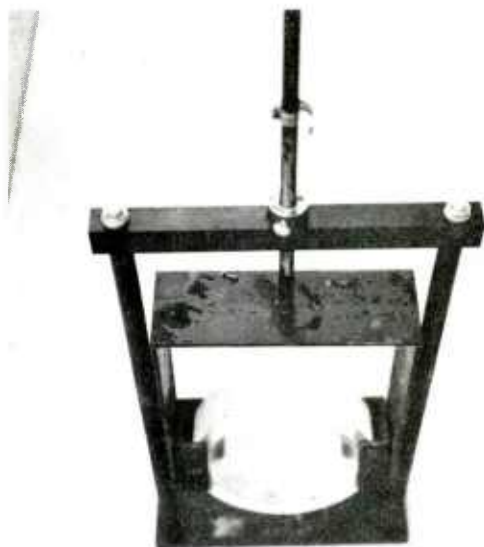
Figure 6. Plexiglas lens and holder.
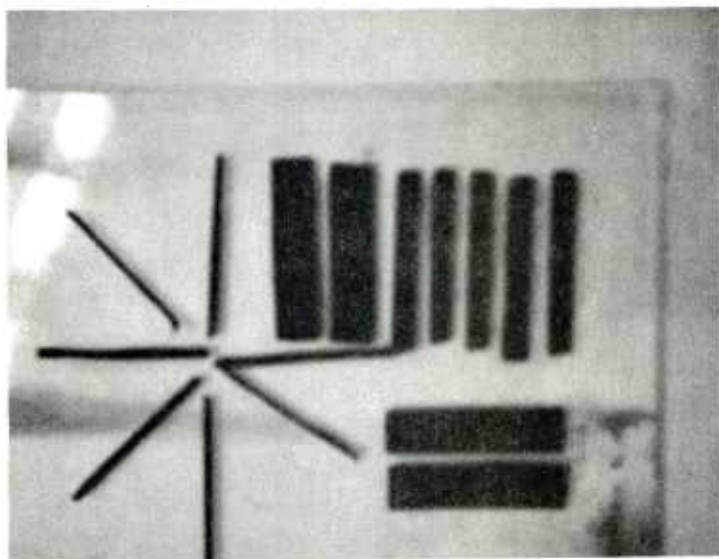
Figure 7. Test target.
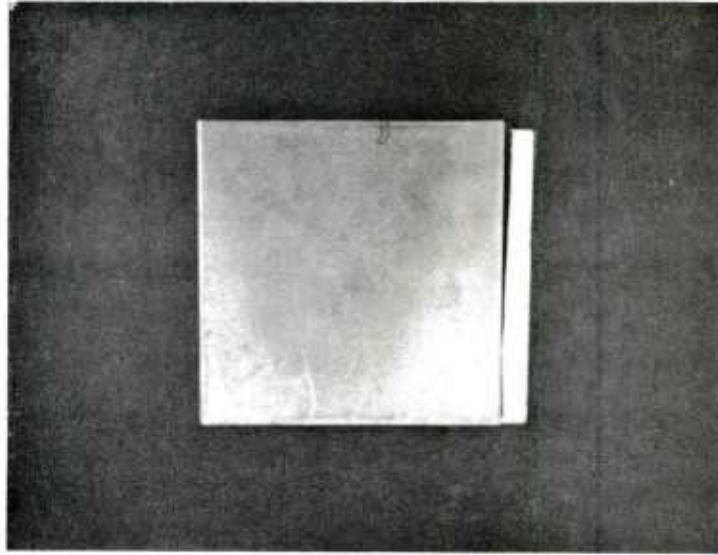
Figure 8.   Flaw model.

$$1/f = (n - 1)(1/R_1 - 1/R_2) \tag{14}$$

where

f   =   lens focal length

R_1 =   radius of curvature of first surface (which is infinite for the plexiglas lens)

R_2 =   radius of curvature for second surface (which is -2.250 inches and -4.5 inches for the two plexiglas lenses)

n   =   index of refraction which is ($v_{water}/v_{plexiglas}$)

v_{water} =   longitudinal velocity of sound of immersion fluid (4,863 ft/sec for water)

$v_{plexiglas}$ = longitudinal velocity of sound in lens material (8,760 ft/sec for plexiglas)

For the 2,250 inches radius lens, the focal length, f, is 5.1 inches. For the 4.50 inches radius lens the focal length, f, is 10.2 inches. The approximate distance of the object and image distance from the lens is calculated from the very familiar thin lens equation

$$1/s + 1/s' = 1/f \qquad\qquad (15)$$

where

s   =   the distance of object from lens and

s'   =   the distance of image from lens.

The performance of the lenses was judged to be an improvement over other lenses. First the field of interference was reasonably uniform, which was not achieved with the other lenses. There appeared to be less distortion of the image with the more rigid plexiglas lens. Of significant note was the increase in resolution when the 5.1 inches focal length lens was used with magnification. The test target hologram is shown in *Figure 9* using the 10.2 inches focal length lens. *Figure 10* using the shorter focal length lens and magnification indicates the increased resolution. *Figures 11* and *12* show the flawed model. The surface tilt as noted in previous reports is very important in being able to "see" the flaw.

It is recommended that improvement in the imaging of flaws can be achieved by image enhancement such as mentioned in imaging some space pictures. This could be incorporated into the system on a real time basis by digitizing the screen image (*Figure 1*), enhancing the image with digital filtering and then playing the information back on a TV screen. The equipment basic to this procedure seems to be available in-house.

To improve the image an acoustical reflector of stainless polished steel was inserted into the system (*Figure 13*). This did improve the image quality and seemed to reduce stray reflections. Steel has a higher acoustic impedance than most other readily available materials such as aluminum, glass or brass. However, tungsten has an acoustic impedance of twice that of steel which depending on availability and cost would make an excellent reflector.

Another item to improve the acoustical system was the use of a freestanding model holder. With the holder pictured in *Figure 14*, a model can be translated in three orthogonal directions very conveniently. The model can also be rotated about the vertical axis to assist in "seeing through" models at critical angles. The frame needs to be a little more rigid. Also a thin
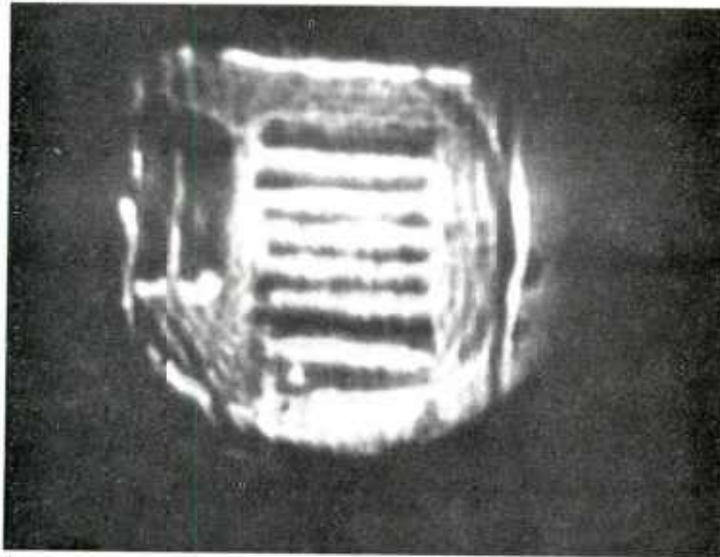
LENS: f = 10.2" S = 24
LASER: 150 MW
OBJ. POWER 3/4
REF. POWER 1/4

Figure 9. Test target acoustical hologram.
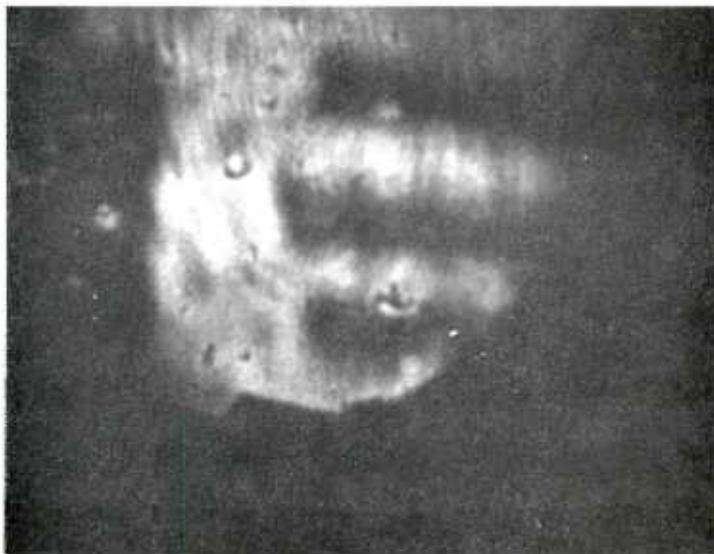
LENS: f = 5.1 S = 7"
LASER: 150 MW
OBJ. POWER 3/4
REF. POWER 3/8

Figure 10. Magnified test target hologram.

LENS: f = 10.2″   S = 24″
LASER: 150 MW
OBJ. POWER 4/4
REF. POWER 3/8

Figure 11.   Flaw model hologram.

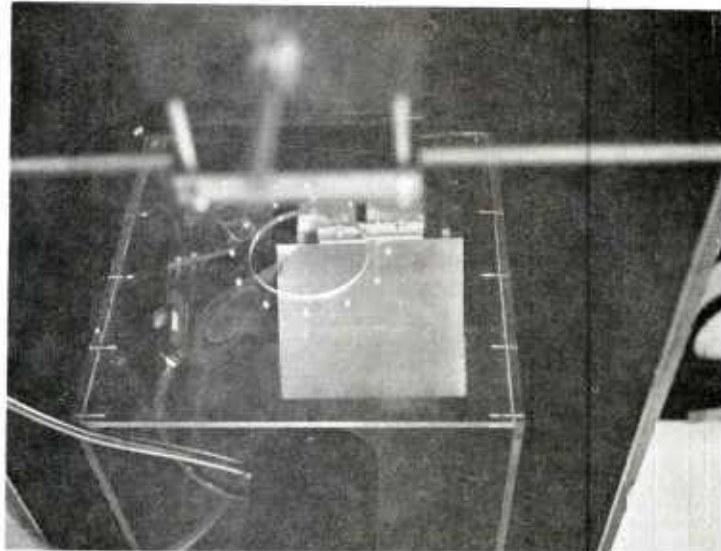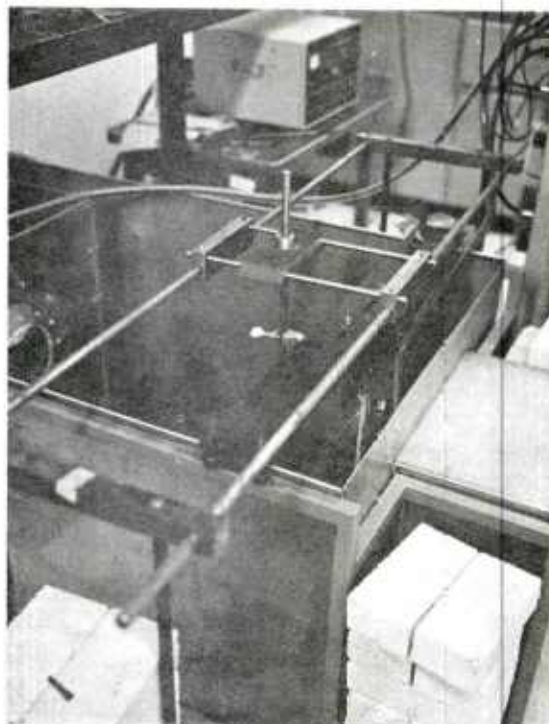**LENS: f = 5.1″   S = 7″**
LASER: 150 MW
OBJ. POWER 4/4
REF. POWER 3/8

Figure 12.   Magnified flaw hologram.

Figure 13. Acoustical reflector.


Figure 14. Model traverse.

membrane over the opening in the isolation tank (*Figure 13*) would help dampen out movement of the model. A thin piece of plexiglas was used in covering the opening but it noticeably absorbed some of the object wave energy.

It should be noted that the acoustical transducers had to be reconditioned. Both transducers were full of immersion fluid from the main tank and as a result did not function properly. The object transducer's inside coating was half gone. The inside coating on one side had flaked off from the crystal. The remaining coating was removed on the inside and a gold coating was deposited. Both transducers were then sealed with a black silicone rubber sealant (*Figure 15*). The transducers have functioned properly since.

Part of this work was centered around attempting to develop a thermoplastic memory device for storing acoustical holograms. The potential of storing acoustical images would open the possibility of using double exposures and quantifying model displacements, internal to the surface as well as on the surface. Eventually this could assist in evaluating surface strains and even subsurface strains. The potential for doing this looks promising even though little apparent success was realized. This technique has been used in optical holography with success and it would appear the techniques could be readily adapted to acoustical holography. Essentially the mechanism for doing this is to have a thermoplastic film in contact with the immersion fluid. At a specified time the film would be heated and softened, allowing the acoustical energy to deform the thermoplastic surface into a holographic diffraction pattern, as is done on the water surface without the film. Next the thermoplastic would be allowed to cool and "lock" in the diffraction pattern for use as a permanent hologram.

Several devices were made and tried. An example of one device is shown in *Figure 16*. A four inch by four inch by .05 inch piece of glass has been coated with indium oxide so current could be passed through the layer. Copper bars were attached to the indium coating with a conducting epoxy. These bars distributed the current so it would flow through the coating. A dam was made of silicone rubber so that thermoplastic could be flowed on the indium oxide coating. The device was leveled. Thermoplastic was dissolved in hexane and poured into the reservoir formed by the silicone rubber dam. When the hexane evaporated, the thermoplastic was distributed over the indium oxide surface. Devices with thermoplastic thicknesses of 0.001, 0.002, 0.003, 0.005 and 0.010 inch were made. The thermoplastic thickness was controlled by knowing the area of the reservoir and the density of the thermoplastic. There is a possibility that some of the thermoplastic was evaporated with the hexane. This, of course, could change the properties of the thermoplastic and would make the amount of hexane, in comparison to the thermoplastic, important. A 20 percent thermoplastic solution was used as well as much higher dilution ratios in some devices. The devices were mounted in the system so
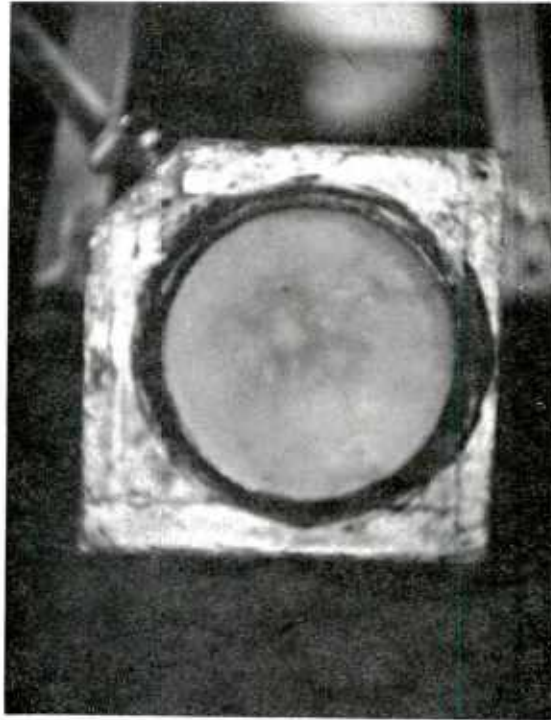
Figure 15.   Sealed transducer.
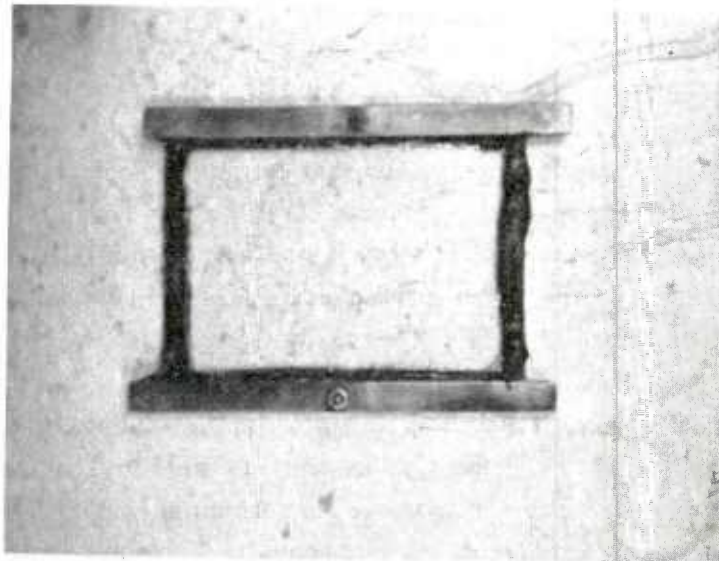
Figure 16.   Resistance heated thermoplastic device.

that the thermoplastic surface was in contact with the water surface and at the water surface. Real time holograms were not apparent with this arrangement. Heat was applied to the device with electric circuits similar to the one illustrated and pictured in *Figure 17*. The temperature of the thermoplastic is very difficult to measure because of the thin layer; therefore, many different heating times were tried from ten milliseconds up to two minutes. The devices were removed and observed in a filter arrangement shown in *Figure 18*. In some instances some extremely questionable images were observed; but nothing that was definite and easily repeatable was seen. One of the biggest problems was obtaining a thermoplastic device with an optically smooth surface. This could have been caused by uneven evaporation of the hexane. After heating, the surface further optically deteriorated obscuring any possible diffraction pattern. This was probably caused by uneven heating and uneven cooling. There is the possibility of using a very thin layer of thermoplastic such as used in optical holography for correcting the uneven heating and cooling. Such a device was made but time was not available to try this approach. The device was made by dipping a plate into solution and carefully controlling the extraction rate. By weighing the device before and after dipping, the film thickness was estimated.

One thermoplastic device was made and heating and cooling applied with hot and cold water but no success was apparent.

Another device was made and is shown in *Figure 19*. This device floated on the surface of the water and was made of plexiglas. The thermoplastic layer was on the inside and was very thick (0.1 inch). The object wave had to pass through the plexiglas and then into the thermoplastic. In this manner a very poor outline could be seen of the test target bars. The reference beam was not received by the thermoplastic. In the arrangement used, the reference beam and plexiglas intersected at an angle greater than the critical angle; thus the reference beam was reflected. No diffraction orders, of course, would be seen. In this arrangement the surface of the thermoplastic was viewed in real time. Some heat was applied using a heat lamp to soften the thermoplastic. Another technique was to pour in a small amount of hexane and let it soften the surface and then evaporate. This was not successful.

An attempt was made at photographing the surface of the water and then filtering the film for the image. The filtering arrangement is illustrated in *Figure 20*. The filtered image of the test target is shown in *Figure 21*. The purpose for such an attempt was to suggest the possibility of doing double exposed holography with acoustics. The double exposure was not tried but with some work this would appear to be feasible. This would allow an investigator to quantify displacements of an object and maybe interior displacement.

Figure 17.   Resistance heating circuit.
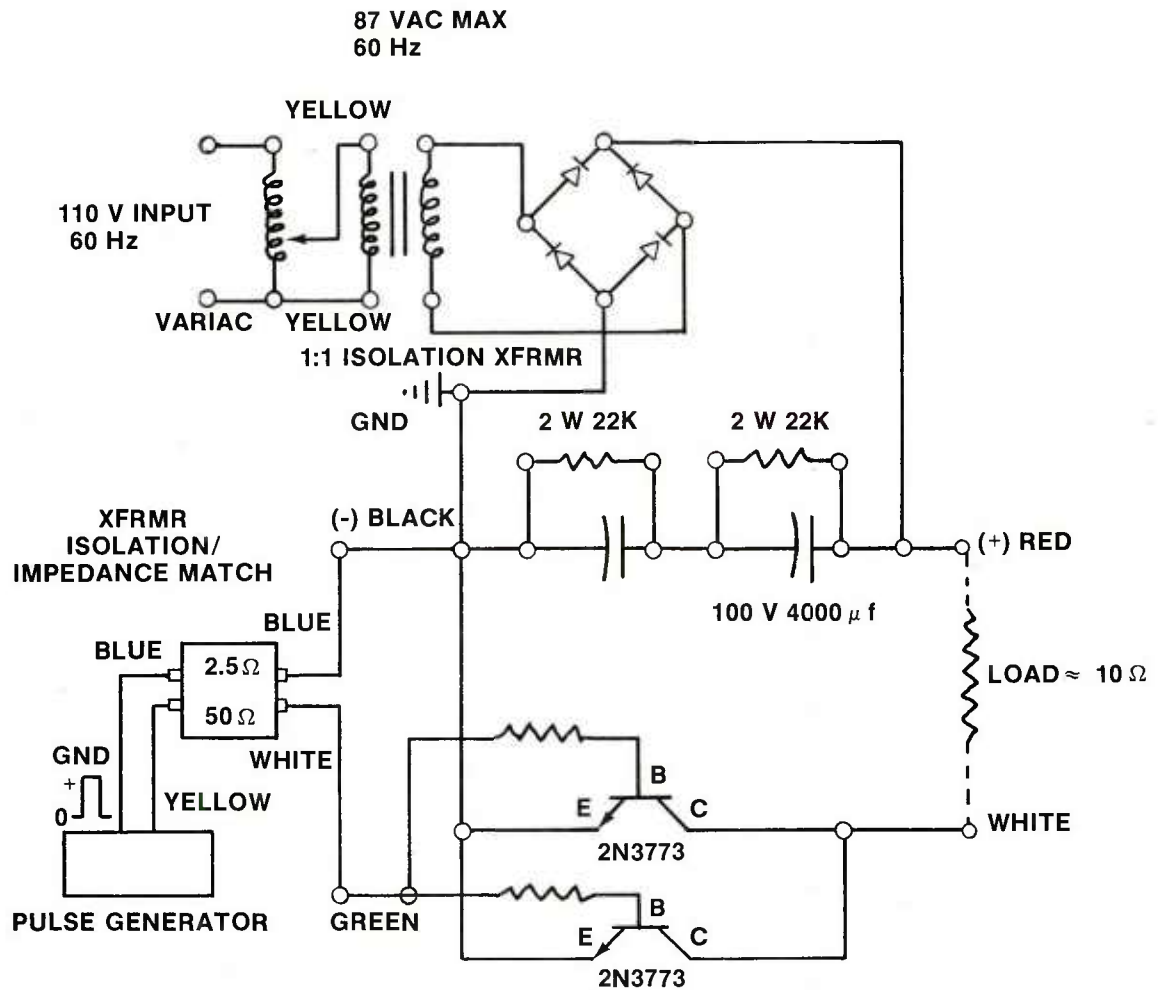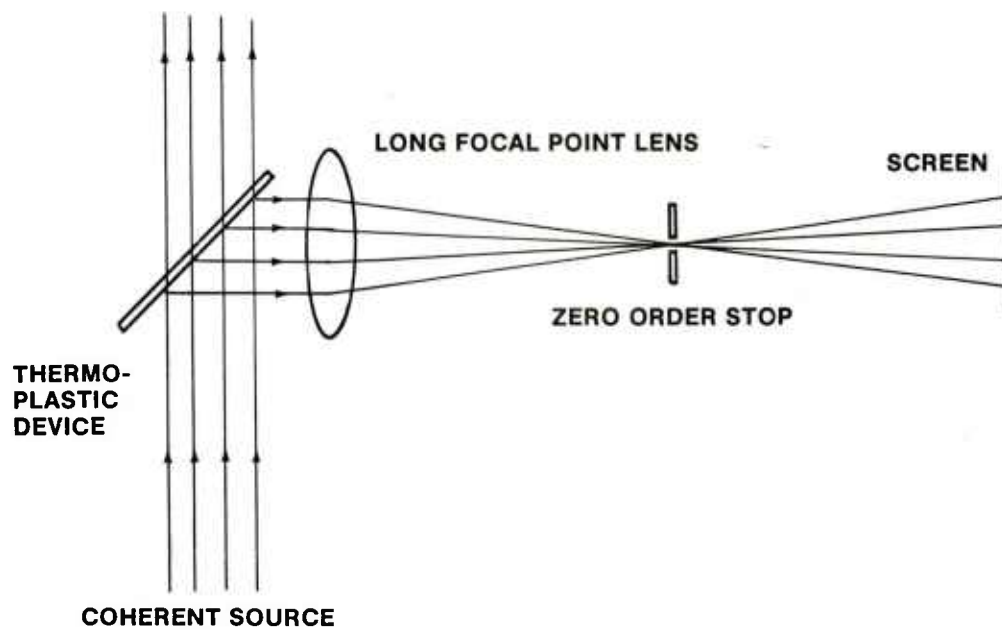
23

Figure 18.   Filtered observation.

Figure 19.   Floating thermoplastic device.

LONG FOCAL POINT LENS

SCREEN

COHERENT LIGHT

FILM

ZERO ORDER STOP
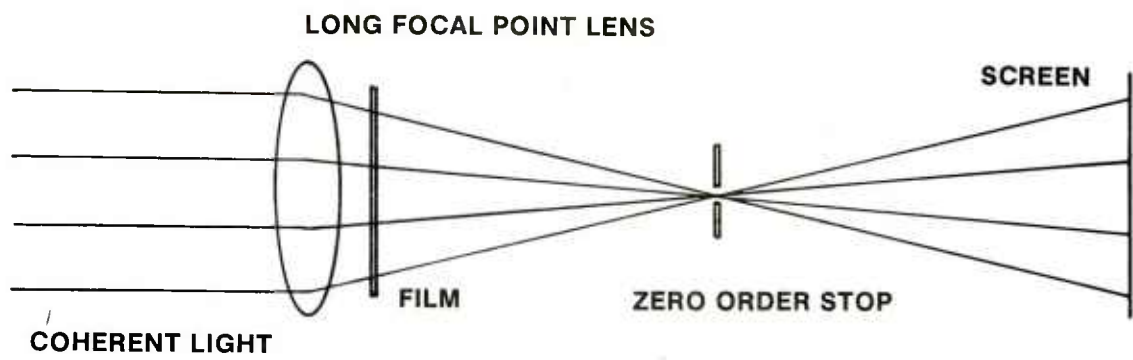
Figure 20.   Film filter system.

Figure 21.   Film record.

An attempt was made to do speckle work with acoustics. A piece of clear plexiglas was inserted into the object beam path. No reference was used. A photograph was made of the water surface. Then the plexiglas was displaced 0.006 inch and a double exposure made. The film was examined using a laser beam of light. At some locations very distinct "Young's fringes" were observed, as shown in *Figure 22*. At other places nothing was observed and still other places strange patterns were seen. This looks very promising. It may require that instead of a laser to examine the film, an acoustic beam would be necessary. It does appear that displacements can be recorded in this manner.

IV. CONCLUSIONS AND RECOMMENDATIONS

The following conclusions and recommendations are made:

1. Pure glycerine as an acoustical immersion fluid is not suitable because of high surface tension. It is recommended that detergent be added to the glycerine and diluted with water as a possible immersion fluid.

2. Plexiglas is a good material for acoustical lenses.
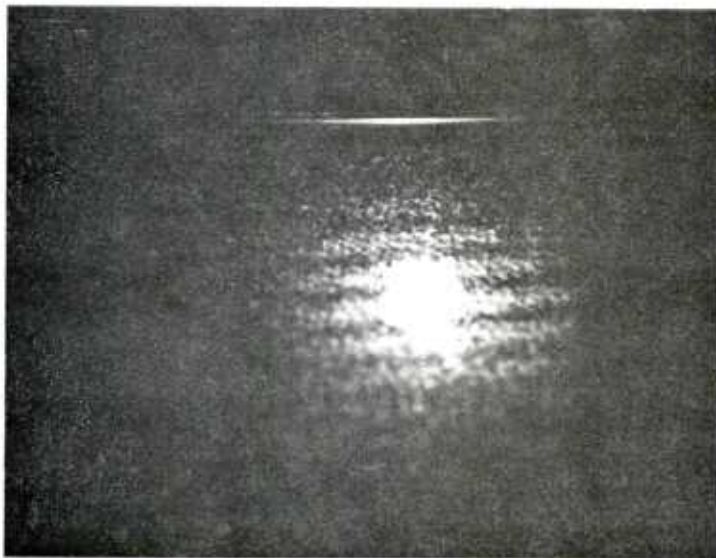
Figure 22.   Acoustical Young's fringes.

3. To improve the acoustical image further, it is recommended that the image be converted to digital form, filtered and enhanced, then converted back to analogue and displayed on a TV screen.

4. If tungsten steel is readily available an improved reflection can be made from this.

5. It is recommended that a thermoplastic memory device with very thin (less than 0.001 inch) coatings be investigated.

6. It is recommended that acoustical speckle be investigated as a possible technique to quantify surface and subsurface displacements.

7. It is recommended that the acoustical ripple pattern on the water surface be photographed using double exposure techniques for possibly recording displacement information.

DISTRIBUTION

No. of
Copies

Defense Technical Information Center
Cameron Station   12
Alexandria, Virginia 22314

Defense Metals Information Center
Battelle Memorial Institute   1
505 King Avenue
Columbus, Ohio 43201

Commander
US Army Foreign Science and Technology Center
ATTN: DRXST-SD3   1
220 Seventh Street, NE
Charlottesville, Virginia 22901

Office of Chief of Research and Development
Department of the Army
ATTN: DARD-ARS-P   1
Washington, DC 20301

Commander
US Army Electronics Command
ATTN: DRSEL-PA-P   1
                -CT-DT   1
                -PP, Mr. Sulkolove   1
Fort Monmouth, New Jersey 07703

Commander
US Army Natick Laboratories
Kansas Street
ATTN: STSNLT-EQR   1
Natick, Massachusetts 01760

Commander
US Army Mobility Equipment
Research and Development Center   1
Fort Belvoir, Virginia 22060

DISTRIBUTION (Continued)

No. of
Copies

Director
USA Mobility Equipment Research and Development Center
Coating and Chemical Laboratory
ATTN: STSFB-CL   1
Aberdeen Proving Ground, Maryland 21005

Commander
Edgewood Arsenal
ATTN: SAREA-TS-A   1
Aberdeen Proving Ground, Maryland 21010

Commander
Picatinny Arsenal
ATTN: SARPA-TS-S, Mr. M. Costello   1
Dover, New Jersey 07801

Commander
Rock Island Arsenal
Research and Development
ATTN: 9320   1
Rock Island, Illinois 61201

Commander
Watervliet Arsenal   1
Watervliet, New York 12189

Commander
US Army Aviation Systems Command
ATTN: DRSAV-EE   1
                -MT, Mr. Vollmer   1
St. Louis, Missouri 63166

Commander
US Army Aeronautical Depot
Maintenance Center (Mail Stop)   1
Corpus Christi, Texas 78403

Commander
US Army Test and Evaluation Command
ATTN: DRSTE-RA
Aberdeen Proving Ground, Maryland 21005

Commander
ATTN: STEAP-MT   1
Aberdeen Proving Ground, Maryland 21005

30

DISTRIBUTION (Continued)

No. of
Copies

Sandia Laboratories
ATTN: Library
P O Box 969   1
Livermore, California 94550

Commander
US Army Air Defense School
ATTN: ATSA-CD-MM   1
Fort Bliss, Texas 79916

Technical Library
Naval Ordnance Station   1
Indian Head, Maryland 20640

Commander
US Army Materiel Development and Readiness Command
ATTN: DRCMT   1
Washington, DC 20315

Headquarters
SAC/NRI (Stinfo Library)
Offutt Air Force Base, Nebraska 68113   1

Commander
Rock Island Arsenal
ATTN: SARRI-KLPL-Technical Library   1
Rock Island, Illinois 61201

Commander (Code 233)
Naval Weapons Center
ATTN: Library Division   1
China Lake, California 93555

Department of the Army
US Army Research Office
ATTN: Information Processing Office   1
P O Box 12211
Research Triangle Park, North Carolina 27709

ADTC (DLDSL)
Eglin Air Force Base, Florida 32542   1

DISTRIBUTION (Continued)

No. of
Copies

University of California
Los Alamos Scientific Laboratory
ATTN: Reports Library   1
P O Box 1663
Los Alamos, New Mexico 87545

Commander
US Army Materiel Development and Readiness Command
ATTN: DRCRD   1
        DRCDL   1
5001 Eisenhower Avenue
Alexandria, Virginia 22333

Director
Defense Advanced Research Projects Agency   1
1400 Wilson Boulevard
Arlington, Virginia 22209

Commander
US Army Research Office
ATTN: DRXRO-PW, Dr. R. Lontz   2
P O Box 12211
Research Triangle Park, North Carolina 27709

US Army Research and Standardization Group (Europe)
ATTN: DRXSN-E-RX, Dr. Alfred K. Nodoluha   2
Box 65
FPO New York 09510

Headquarters
Department of the Army Office of the DCS for Research
   Development and Acquisition
Room 3A474, The Pentagon
ATTN: DAMA-ARZ   2
Washington, DC 20310

US Army Materiel Systems Analysis Activity
ATTN: DRXSY-MP   1
Aberdeen Proving Ground, Maryland 21005

IIT Research Institute
ATTN: GACIAC   1
10 West 35th Street
Chicago, Illinois 60616

DISTRIBUTION (Concluded)

	No. of Copies
DRSMI-LP, Mr. Voigt	1
DRSMI-R, Dr. Kobler	1
-RL, Mr. Lewis	1
-RLA, Mr. Pettey	1
-RLA, Dr. Mullinix	1
Mr. Schaeffel	50
-RT	1
-ICBB	1
-RPR	3
-RPT (Record Set)	1
(Reference Copy)	1